Scientific African 24 (2024) e02207

Contents lists available at ScienceDirect

Scientific African

journal homepage: www.elsevier.com/locate/sciaf

A comprehensive analysis and future projection of land use and land cover dynamics in a fast-growing city: A case study of Sekondi-Takoradi metropolis, Ghana

Ernest Biney [a,b,*], Eric Kwabena Forkuo [a,b], Michael Poku-Boansi [c], Yaw Mensah Asare [b], Kwame O. Hackman [d], Daniel Buston Yankey [b], Albert Elikplim Agbenorhevi [e], Ernestina Annan [a]

[a] WASCAL Graduate Research Programme on Climate Change and Land Use, Department of Civil Engineering, Kwame Nkrumah University of Science and Technology, Kumasi, Ghana
[b] Department of Geomatic Engineering, Kwame Nkrumah University of Science and Technology, University Post Office Box PMB, Kumasi, Ghana
[c] Department of Planning, Kwame Nkrumah University of Science and Technology, Kumasi, Ghana
[d] Data Management Department, WASCAL Competence Center, Ouagadougou, Burkina Faso
[e] WASCAL Climate Change and Water Resources, Université d'Abomey-Calavi, Benin

ARTICLE INFO

Editor: DR B Gyampoh

Keywords:
Land use and land cover
Landsat images
Geospatial techniques
Land compositions
Random forest
Sustainable development goals

ABSTRACT

Sekondi-Takoradi is the most urbanized metropolis in the Western region of Ghana. Over the past two decades, it has experienced rapid shifts in both population density and land cover. Unfortunately, these transformations have significantly altered the natural landscape and expanded urban coverage. Previous studies have not established enough evidence on land use and land cover changes in the metropolis. For this reason, this study examined the existence, rate, and spatial distribution of land use and land cover as well as the future changes in land cover in the metropolis. Landsat imagery spanning from 1991, 2009, 2016, to 2023 provided the basis for evaluating the spatiotemporal dynamics of land use and cover within the metropolis. The Random Forest Classification algorithm was employed to categorize the images into three distinct classes: water, vegetation, and built-up areas. Analysis revealed a rapid growth in built-up areas by 63.08 km^2 (32.91 %), accompanied by a decrease in vegetation and water coverage by 60.99 km^2 (31.82 %) and 2.08 km^2 (1.09 %) respectively. This highlights the accelerating urbanization trend, emphasizing the critical need for vigilant monitoring and controlled urban expansion to mitigate potential adverse effects. Projections for 2030 indicate further changes with water areas decreasing to 1.21 km^2 (0.63 %), vegetation diminishing to 95.31 km^2 (49.73 %), and built-up areas expanding to 95.14 km^2 (49.64 %). This signifies a significant shift towards built-up areas, altering the metropolis' land cover composition and potentially impeding the achievement of Sustainable Development Goal 11. Understanding these changes in land use and land cover holds significant value for policymakers, enabling them to effectively monitor and safeguard natural resources.

* Corresponding author.
E-mail address: ernest_biney@yahoo.com (E. Biney).

https://doi.org/10.1016/j.sciaf.2024.e02207
Received 20 September 2023; Received in revised form 8 February 2024; Accepted 3 April 2024
Available online 4 April 2024

Introduction

Globally, more than 70 % of the changes that occur on the land surface are human-induced [1]. Unfortunately, these changes, especially the conversion of vegetation and waterbodies to built-up areas have little chance of being restored to their former cover [2]. As a result, the decision to put land to a particular use must be carefully assessed before any action is taken to avoid manifold dire implications [3]. According to Ramadan & Effat, [4], and Krishnaveni & Anil, [5], anthropogenic activities that bring changes in the land use land cover are mostly fueled by population growth and increasing economic activities. Currently, the world's population stands at 8 billion with an annual growth rate of 1.11 % [6]. About 55 % of the world's population resides in urban areas and this figure is estimated to increase to 68 % by 2050 [7,8]. Also, urban cities with a population exceeding 1 million are expected to increase from 512 to 662 cities by 2030. This growth will force the acquisition of more land and accelerate competition in land use [1]. Land use reflects human activities such as the use of land for different purposes whereas land cover refers to the physical condition or the biophysical state of the earth's surface [9]. The actions of people in their environment directly affect the land cover, i.e. land use may lead to land cover change [10]. Therefore, Aduah & Baffoe, [11] argue that when transformations in urban areas are not adequately managed they can lead to numerous social, economic, and environmental problems. Africa, for instance, is experiencing a high rate of urban growth, but it is characterized by unplanned urbanization which is shown in the imbalance between the level of urbanization and its economic and industrial growth [12]. Despite urban areas occupying a relatively small portion of land size compared to other land cover types, the swift expansion of urban areas around the world, especially in Africa, due to the pressure on the land, is causing transformations in the land cover classes such as vegetation, farmland, forests, wetlands, and waterbodies [13–16]]. Krishnaveni & Anil, [5], further assert that in developing countries, urban development and land cover changes are often driven by a combination of socioeconomic, environmental, and institutional factors. These factors regrettably cause significant challenges such as informal settlements and slums, inadequate infrastructure, lack of adequate housing, land degradation, inequality and social exclusion, and climate change vulnerability [17,18].

In Ghana, urban expansion primarily involves extensive and unrestricted outward growth, often at the expense of other land cover types [19,20]. From 1975 to 2010, Ghana witnessed a significant increase in its urban areas from 2560 km^2 to 3830 km^2 [21]. Unfortunately, this rapid urbanization has led to the conversion of various land cover into residential and industrial areas. A report by the Sekondi-Takoradi Metropolitan Assembly (STMA), asserts that the metropolis is experiencing a surge in socio-economic activities, with multiple infrastructural projects across various sectors [22]. This increase intensified after the 2010 oil discovery in Ghana, drawing a notable influx of people and a surge in real estate activity [23,22]. In this regard, between 2010 and 2013, the spatial development planning unit of Sekondi-Takoradi emphasized the changing landscape due to development pressures [22–25]. These changes pose challenges to the city's sustainability, conflicting with global development goals for inclusive, safe, and resilient cities by 2030, particularly SDG 11 [26]. Research work by Biney & Boakye, [27] and Mensah et al., [22], reveals that the metropolis is experiencing an excessive increase in built-up and a rise in impervious surfaces. Such high levels of impervious surfaces are not recommended in sustainable cities due to their runoff potential, limited infiltration capacity, and low reflection of solar radiation. In this light, Aduah & Baffoe, [11], assert that if changes in urban areas are not properly handled, they can result in tragedies that will affect the livelihood of urban dwellers and consequently destroy the sustainable development of urban lands. Fortunately, Sekondi-Takoradi is a business hub for local, national, and international organizations, therefore, any disaster in this area would have ripple effects on the national and to some extent the global economy.

Land use and land cover change (LULCC) can be monitored by the help of different geospatial techniques. Geographic Information Systems (GIS) and Remote Sensing (RS) have emerged as widely employed geospatial techniques for detecting changes in land use and land cover [14,19,28–32]. For instance, through the analysis of satellite images, land cover transformations have been measured effectively and accurately compared to the traditional survey method [33]. This viewpoint is supported by Dissanayake, [34,35], and Rana & Sarkar, [36] as their studies demonstrated that using remote sensing and GIS to analyze the rate of land cover transformation is a time-efficient and cost-effective method. In recent times, addressing the potential future LULC changes has gained international attention, therefore, various spatiotemporal prediction models, including the Markov chain (MC) model, the Cellular Automata (CA) model, and the conversion of land use and its effects (CLUE) model, have been developed to forecast land use and land cover changes (LULCC) [37]. Among these, the CA model has been widely employed in spatio-temporal dynamic modeling for land-use change analysis. MOLUSCE (Modules of Land Use Change Evaluation), a QGIS plugin, utilizes the CA model to estimate potential LULC changes. This plugin employs four established algorithm models: Artificial Neural Networks (ANN), Logistic Regression (LR), Multi-criteria Evaluation (MCE), and Weights of Evidence (WoE). Within MOLUSCE, the CA-ANN model serves as a reliable tool for predicting future LULC changes, offering valuable insights for land use planning and management. This approach is particularly effective for forecasting future LULC scenarios [38]. In this context, GIS and remote sensing techniques were used to analyze the dynamics of land use and land cover of Sekondi-Takoradi Metropolis, and the CA-ANN model was utilized to predict the future LULC for the year 2030.

This study will contribute to elucidating the increasing concerns of land cover changes in the Metropolis, and the negative consequences it has incurred over the study years. Therefore, city planners and policymakers will gain a comprehensive understanding of the multifaceted aspects and spatio-temporal dynamics of land use and land cover which will enable them to allocate resources efficiently and implement effective infrastructure management strategies accordingly. Also, the approach employed in this study can also be used to evaluate urban growth in other cities in Ghana or other developing nations with comparable conditions. The extent to which this study area's land use and land cover has been studied in terms of its pattern, magnitude, rate, and spatiotemporal characteristics as well as its effects on the other LULC categories is lacking. It is against this background that this study aims to analyze the dynamics and future projection of land use land cover in the metropolis over the past 32 years (from 1991 to 2023). This paper is

structured mainly as follows: The first section gives a general overview of urban expansion; the second section describes the materials and methods which includes the study area descriptions, data types and software used, and method of data analysis; the third section presents the results and discussions; and the fourth and final section presents the conclusion of the study. Nevertheless, some of the major sections are further divided into subsection headings.

Materials and methods

The study's methodology has been sub-sectioned into 1. Study area (Fig. 1) 2. Materials: Dataset used and Software 3. Method: this includes image pre-processing, selection of training and validation, image classification, accuracy assessment, and land use and land cover change analysis (Fig. 3).

Study area

The Sekondi-Takoradi Metropolis lies between latitude 4° 52′ 30″ N and 5° 04′ 00″ N and longitudes 1° 37′ 00″ W and 1° 52′ 30″W. The Metropolis is bordered by Ahanta West District at the west, Shama District at the east, the Atlantic Ocean at the south, and Wassa East district at the north [39]. It is also the administrative capital of western region and has an area size of about 191.7 km^2. According to the Population and Housing Census (PHC) of 2021, the population of the metropolis has increased to 734,645 (Ghana Statistical Service, 2021; [40]). With this increasing population, 96.1 % live in urban localities, and 3.9 % live in rural localities [41,42]. This proves that a large number of the people living within the metropolis live in urban areas. Industries such as timber, plywood, ship-building, railway repair, and oil industries are major industries found in Sekondi-Takoradi [22,43]. The metropolis has two main rivers; Whin River and Kansaworado River [11]. The climate of the Metropolis is equatorial, with an average annual temperature of about 22 °C, experienced between January and March. Rainfall is bi-modal, with the major season occurring between March and July and the minor season occurring between August and November. The mean annual rainfall is about 1380 mm, covering an average of 122 rainy days. [43]. A pictorial description of the study area can be seen in Fig. 1.

Datasets used and software

The data used for the study is shown in Table 1. They are categorized into Landsat image and referenced data. The Landsat images utilized in this study were downloaded from the United States Geological Survey (USGS) Earth Explorer and with a criterion of images having less than 10 % cloud cover. The study area falls within path 194 and row 057 of the Worldwide Reference System (WRS2). Given the study's extensive scope, the Landsat images were obtained from different Landsat sensors (Table 1). The Scanline errors in the 2009 and 2016 Landsat 7 ETM+ images (Fig. 2) were rectified through a gap-filling process in Quantum Geographic Information System (QGIS.3.22). Moreover, the images were acquired in the same season for each year to avoid extreme differences in the land cover reflectance dataset. Four images were used for the study to have a better understanding of how the land cover has changed over the years, however, the inconsistency in the image intervals was due to the lack of data with a cloud cover of less than 10 %. Reference

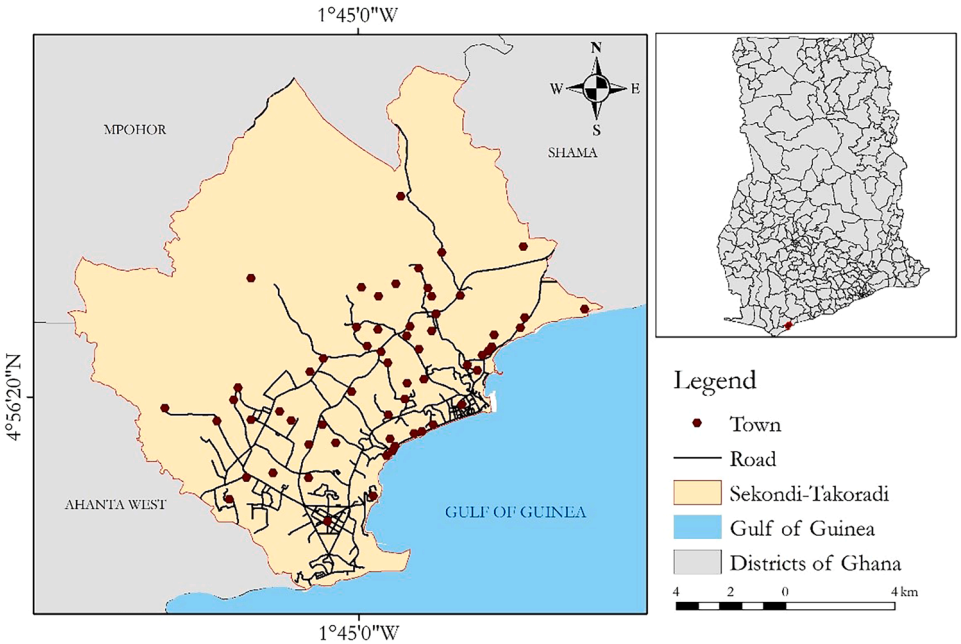

Fig. 1. Map of the study area.

Table 1
Dataset used for the study.

Landsat image	Resolution	Date acquired	Source	No. of bands
Landsat TM	30 m	01/01/1991	USGS	7
Landsat ETM+	30 m	01/02/2009	USGS	8
Landsat ETM+	30 m	06/01/2016	USGS	8
Landsat OLI/TRIS	30 m	01/01/2023	USGS	11
Reference data				
Google Earth images		1991, 2009, 2016 and 2023	Google earth explorer	
Land cover maps		1991, 2009,2016	Forestry Department, Ghana	
Spatial variables (DEM, Slope, Proximity to road and city center)	30 m		USGS/Survey Department	

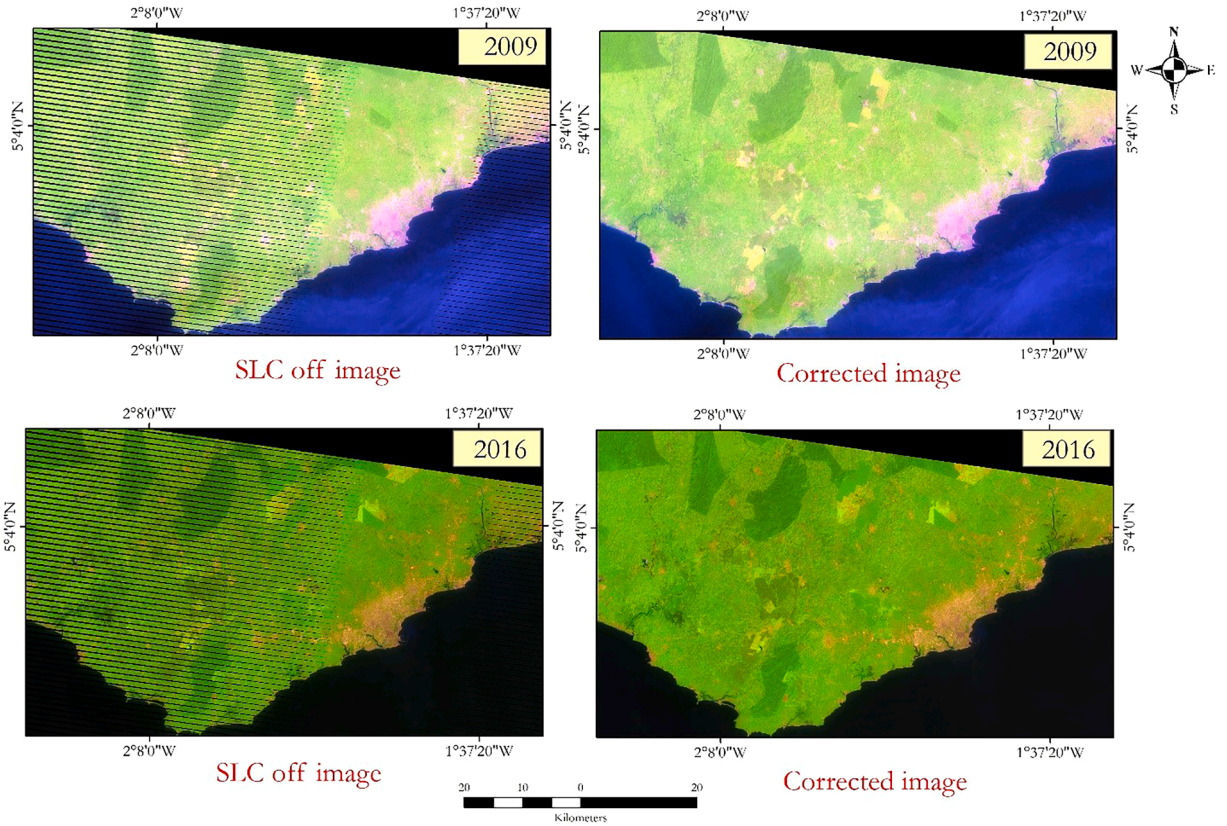

Fig. 2. SLC off and corrected image of Landsat 7.

data were gathered from a variety of sources (Table 1). Google Earth images, GPS points, and land cover maps were used in training and assessing the accuracy of the classification. Using the stratified random sampling technique, 1200 Ground Control Points (GCPs) were selected. Out of these, 840 (70 %) were allocated for training, while the remaining 360 (30 %) were set aside for validation.

The Landsat images were pre-processed and processed using several software such as Google Earth engine, QGIS, and ArcGIS Pro. The QGIS and Google earth engine were used specifically to pre-process, classify, and assess the accuracy of the satellite images. ArcGIS Pro-was used to produce all classified and output maps whereas the generation of change maps, transitional probability, and modeling and predicting future changes in the land cover were done using QGIS.

Methods

The method employed in this study is primarily categorized into four stages. These stages are Image Pre-processing, Image classification, Change Detection, and Modelling and Prediction of land cover change. A flow chart outlining the study's approach is shown in Fig. 3.

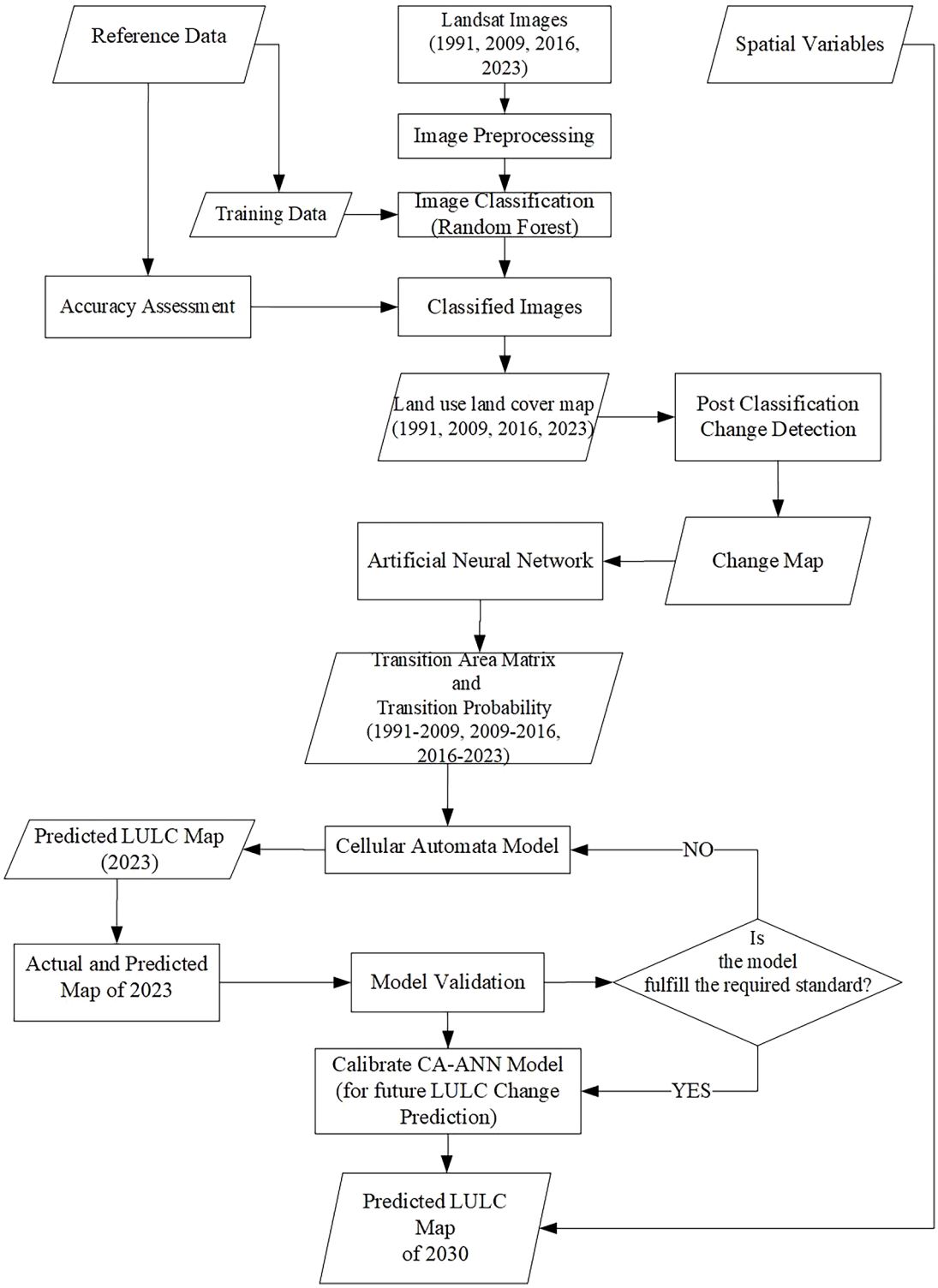

Fig. 3. Methodological flowchart of the study.

Image pre-processing

Satellite images need to be pre-processed to correct any errors caused by atmospheric influence, earth curvature, and sensor effects before image classification and change detection can be done efficiently [44]. The image pre-processing that was conducted in this study were geometric corrections, radiometric corrections, and image band stacking. The acquired Landsat images were geometrically

corrected from source and geo-referenced to 1984 World Geodetic System Universal Transverse Mercator Zone 30 North Projection (UTM '84 zone 30 N). However, to ensure uniformity in the size and position of the acquired images, image-to-image registration was performed in QGIS using 2023 Landsat image as the reference image and then were reprojected to UTM '84 zone 30 N [45]. The radiometric correction performed on the images was carried out in QGIS by using the Semi-Automatic Classification (SCP) plugin. The bands of the Landsat images used in this study range from 1 to 11. These bands were combined to form a multi-colour band and displayed in different colour band combinations. A False Colour Composite (FCC) was used to identify the land cover classes on the images for classification. The FCC was chosen because it produced distinct spectral signatures for easy identification of land cover classes such as water, vegetation, and Build-up which is needed for analysis [46].

Image classification

One of the most important steps in extracting important information from satellite images is image classification [18]. In this study, the classification was done by first acquiring training samples, creating training sites, and employing the supervised classification technique. There are several supervised classification techniques available [44], but the study used the random forest supervised classification method to classify the images because it yields results with excellent accuracies and can work efficiently on large datasets with higher noise levels [47,48]. This has been proven in the works of Fernández-Delgado,[49], who evaluated 179 relevant classifiers from 17 families using 121 datasets and found random Forest to be the best classifier. Also, Random Forest is useful in calculating important information about errors, variable importance, and data outliers. Such information can be used to assess the performance of the model and make changes to the training data if necessary [50]. The training samples were acquired from Google Earth images and GPS coordinates during field visits. In line with the objective of the study, the study area was classified into three classes, as explained in Table 2.

Accuracy assessment

After pre-processing and image classification, the process of determining the accuracy of the classified images was carried out. This process is crucial because classification with inaccuracies will misguide the analysis of land use land cover [2,51]. In this study, a validation dataset was used to assess the performance of the classified images. The validation dataset was obtained from high-resolution satellite images such as the Google earth and from field surveys. Since the validation dataset used to assess the accuracy of the classification must be collected in the same period as the classified data [44], the study used validation dataset that correspond to the exact years of the classified images. The points for validation were randomly selected over the study area with samples for each class not less than 100 points. A total random point of three hundred for each year was extracted to perform the accuracy assessment. Using the confusion matrix, the accuracy of the classification results was assessed [52]. Various measures such as overall accuracy, kappa coefficient, user's and producer's accuracy were computed from the confusion matrix [45,53]. The accuracy assessment parameters used in the classification accuracy can be expressed mathematically in the following Eqs. (1-4) [54].

$$User\ Accuracy = \frac{Number\ of\ correctly\ classified\ pixels\ in\ each\ category}{Total\ number\ of\ classified\ pixels\ in\ that\ category\ (the\ row\ total)} \times\ 100 \tag{1}$$

$$\text{Producer Accuracy} = \frac{\text{Number of correctly classified pixels in eacg category}}{\text{Total number of classified pixels in that category (the column total)}} \times\ 100 \tag{2}$$

$$Overall\ Accuracy = \frac{Total\ number\ of\ correctly\ classified\ pixels\ (Diagonal)}{Total\ number\ of\ reference\ pixels} \times\ 100 \tag{3}$$

$$Kappa\ Coefficient = \frac{(TS \times TCS-) - \sum (Column\ Total \times Row\ Total)}{TS2 - \sum (Column\ Total\ \times Row\ Total)} \times\ 100 \tag{4}$$

Where TS is the Total number of samples and TCS is the Total number of correctly classified samples.

Change detection

In this study, a post-classification change detection was used to analyze the changes in the land cover [55]. The reason for using the post-classification change detection is that it provides comprehensive information on changes that occur in a class cover to other classes concerning the place of change, the extent and the amount of the change [13,22,56]. This, according to Asare et al., [57], makes it possible to have a change matrix, which helps to track any change in pixel between two time periods to ascertain the trade-offs

Table 2
A land cover classification scheme.

land cover class	Explanation
Water	This includes the rivers, streams, and lakes, inland water in the study area.
Vegetation	This includes farmlands/ agricultural lands and forest areas.
	Land used primarily for the production of food and fibre, cropland, pasture, and other commercial and horticultural crops
Built-up or Settlement	This includes built-up areas or areas covered by made-made structures, impervious surfaces, residential areas, industrial areas, and commercial areas, paved areas, roads.

Source: Modified from Anderson Classification system, (1980).

between the classes. Based on the classified images, the post-classification change detection was conducted in QGIS. This involved computing the change statistics and generating change maps for the time steps (1991–2009, 2009–2016, 2016–2023, and 1991–2023) to determine changes that have occurred within the metropolis. Also, as part of the post-classification change detection, the annual rate of change and percentage annual rate of change were computed using Eq. (5) and (6) respectively [12,19,58–60].

$$A_r = \left(\frac{A_2 - A_1}{T}\right) \tag{5}$$

Where A_r is the annual rate of change, A_2 is the current area of land use and land cover type in km^2 and A_1 is the initial area of land cover type in km^2, and T= time interval between initial year (A_1) and the current year (A_2).

$$C = \left[\left(\frac{F - I}{I}\right) * \left(\frac{1}{T}\right)\right] * 100 \tag{6}$$

Where "C" is the percentage annual rate of change, "F "is the final year, "I" is the initial the year, "T" is the time period (interval) between the final year and the initial year.

Change transition and prediction of land use and land cover

In this study, the cross-tabulation matrix was used to determine the growth and changes between all land use and land cover maps. According to Abdullahi & Pradhan, [61], the output of cross-tabulation can be in four types, namely: 1. cross-classification image, 2. full cross-tabulation table, 3. both cross-classification image and cross-tabulation table, and 4. image similarity data only. To have a cross-tabulation table and cross-classification image, output type 3 was chosen for this study. Using the MOLUSCE matrix module in QGIS, four cross-tabulation tables from the classified maps 1991–2009, 2009–2016, 2016–2023, and 1991–2023 were produced for this study. Within the tabulation table, the elements in the diagonal positions represent classes that have not changed, whereas the off-diagonals represent classes that have changed. The horizontal elements indicate classes in a later time period (second year), while the vertical elements indicate classes in an earlier time period (first year). The last rows and columns of the tables are the total of each row and column and they indicate either a loss or gain for the various classes or land use categories. Growth occurs when there is a positive value and loss occurs when there is a negative value. According to Boakye et al., [62], a predicted land cover type can be computed by the cellular automata predicting model. For the projection of land cover maps, the Modules for Land Use Change Evaluation (MOLUSCE) plugin software in QGIS was used to project future land use and land cover map of 2030. The model parameters used in the MOLUSCE for the simulation are Iteration rate: 1000, Learning rate: 0.001, Momentum: 0.02, Neighbourhood: 10px, Hidden layer: 10, and model iteration was set at 14 [14,38,63]. Researchers such as [14,37,57,64–66] have used MOLUSCE to forecast future land use and land cover maps. The MOLUSCE employs cellular automata (CA) to predict future land cover maps and artificial neural networks (ANN) to simulate changes in land cover from one class to another [66]. Furthermore, MOLUSCE computes Pearson's correlation between spatial variables of land cover class and the likelihood that each land cover class will transition to another land cover class.

Results and discussion

To better comprehend the land cover changes in Sekondi-Takoradi Metropolis for the years 1991, 2009, 2016, and 2023, the results are presented separately as classified land use and land cover, accuracy assessment, transition matrix, spatial variables, and prediction of land use and land cover.

Classified land use and land cover maps

By visual interpretation of Fig. 4, built-up areas increased significantly throughout the study periods while water and vegetation decreased over the years. A detailed statistical account of Fig 4 which comprises the total land area, area and percentage cover of each class for the various years is presented in Table 3.

From Table 3, the total area coverage of water in the year 1991 was 3.38 km^2 (1.77 %) and it decreased to 2.21 km^2 (1.16 %) in 2009. This decrease in water further decreased to 1.03 km^2 (0.54 %) in 2016 but later increased in 2023 to 1.30 km^2 (0.68 %). The water body decreased by 1.17 km^2 (0.61 %) from 1991 to 2009, again decreased by 1.18 km^2 (0.67 %) during 2009–2016, and then increased by 0.23 km^2 (0.14 %) during 2016–2023 (Table 4). The decrease in water during the periods of 1991–2009 and 2009–2009 can be attributed to a substantial increase in infrastructural development or build-up [22,23,67]. This result corroborates the assertions of Mosammam et al., [68] and Wangyel et al., [32] that the expansion of built-up can have detrimental implications on the area coverage of water, especially, if not properly monitored. However, the increase in water was due to the consecutive flooding incidents that occurred in the years 2019, 2021, 2022, and 2023. In those years mentioned, several flood-prone areas experienced inundation. For instance, the Wetlands near New Takoradi and the Aboadze thermal plant, and areas near the Whin River experienced inundation as the banks of the river were breached, hence, leading to the submersion of numerous hectares of diverse land cover [41]. In General, the area of water was reduced by 2.08 (1.09 %) between 1991 and 2023 as a result of the conversion to other land use and land cover classes primarily built-up as indicated in Fig. 4 and Table 3. This suggests that people have encroached upon water areas for construction purposes. These waterways are often filled with sand and prepared for building and other construction activities. In the study of Aduah & Baffoe, [11] it was revealed that the waterways and waterbodies within the metropolis were being converted into built-up

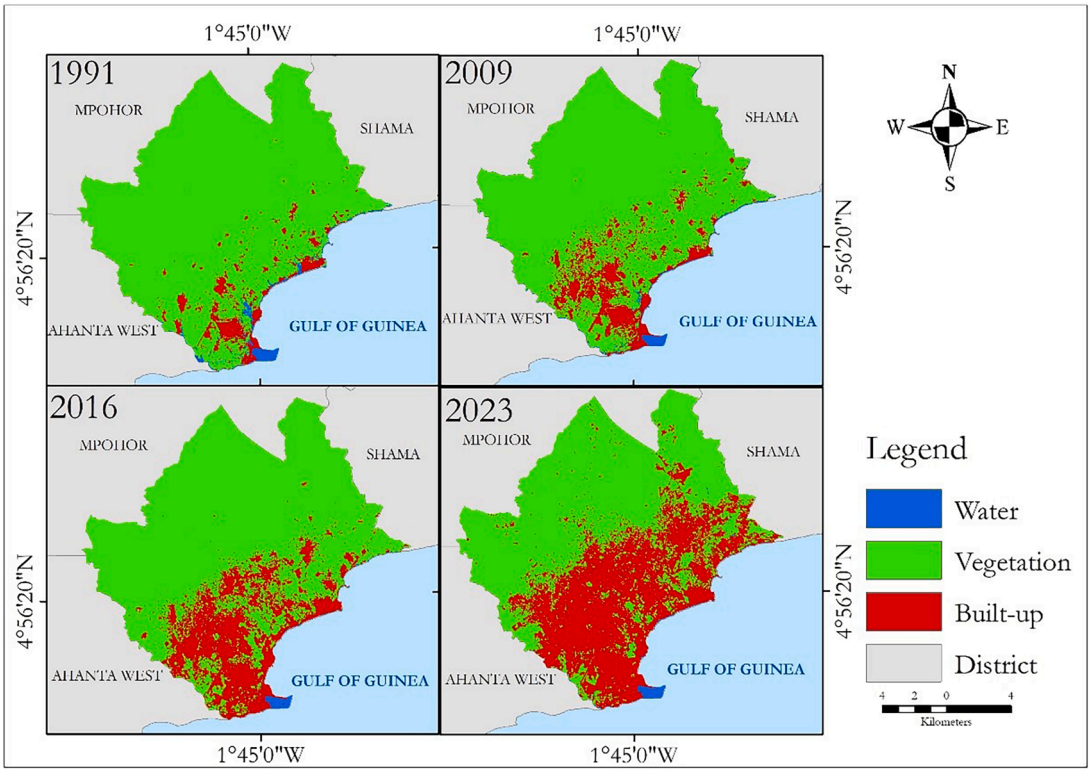

Fig. 4. land use and land cover (LULC) maps from 1991 to 2023.

Table 3
Area statistics of land cover classes from 1991 to 2023.

Class	1991		2009		2016		2023	
	Area (km^2)	(%)	Area (km^2)	(%)	Area (km^2)	(%)	Area (km^2)	(%)
Water	3.38	1.77	2.21	1.16	1.03	0.54	1.30	0.68
Vegetation	177.72	92.72	167.32	87.29	151.66	79.13	116.73	60.90
Built up	10.56	5.51	22.13	11.55	38.98	20.33	73.63	38.42
Total	**191.66**	**100**	**191.66**	**100**	**191.66**	**100**	**191.66**	**100**

areas. Additionally, Dadzie-paintsil & Mensah, [41], revealed that residents in communities such as New Takoradi, Kojokrom, Buabakrom, and Whindo in the metropolis have encroached upon portions of the water bodies. A notable example is the Anankori River, where certain tributaries have been obstructed and filled with boulders to facilitate the transportation of quarry materials via heavy-duty trucks [27,69]. The state of these water bodies and channels compared to the 1990s signifies a high rate of encroachment and conversion into built-up which will deprive the metropolis of enjoying the benefits associated with water conservation [70].

Area coverage of vegetation in 1991 was 177.72 km^2 (92.72 %) and this reduced to 167.32 km^2 (87.29 %) in 2009. As witnessed in the previous year (2009), vegetation continued to decrease to 151.66 km^2 (79.13 %) in 2016 and to 116.73 km^2 (60.90 %) in 2023 (Table 3). Throughout the entire timeframe, the area occupied by the vegetation class continuously reduced. It experienced a reduction of 10.40 km^2 (5.43 %) from 1991 to 2009, followed by a further decrease of 15.66 km^2 (8.16 %) between 2009 and 2016. Subsequently, there was an additional decline of 34.93 km^2 (18.23 %) between 2009 and 2023 (Table 4). Overall, from 1991 to 2023, the vegetation class consistently decreased, by 60.99 km^2 (31.82 %) which is mainly due to the transformation of vegetation to built-up as seen in Fig. 4. This outcome is in agreement with the notion that when the urban area is expanding the vegetation class become the prime target [71,72]. According to the Ghana Statistical Service (2015), the Sekondi-Takoradi metropolis has experienced a significant influx of migrants since 1991. This population growth has exerted pressure on the available green spaces, leading to the conversion of lands within and beyond the urban fringe for various purposes by individuals and private estate developers. A study conducted by Mensah et al., [73] on urban green spaces in Sekondi-Takoradi revealed ongoing building projects at different stages of construction encroaching upon vegetative land and semi-natural green spaces. Within the metropolis, the Monkey Hill nature reserve, and the Whin Estuary, serve as prominent examples of semi-natural urban green spaces. These semi-natural green spaces are currently facing rapid encroachment due to population pressure, and so, pose a significant risk of diminishing the benefits such as preserving biodiversity,

acting as carbon sinks, and supporting eco-tourism derived from these spaces. Further, the Independent Oil and Gas Information Centre [74], revealed that about 49,000 people working in the oil and banking sectors are seeking for housing within the metropolis. This substantial demand for housing has incentivized landowners, predominantly chiefs and family members due to the customary land tenure system in Ghana [75], to sell off green spaces to capitalize on the lucrative housing market [76]. This situation aligns with the social disruption theory, which argues that the discovery of oil leads to the breakdown of social systems [77]. In the case of the metropolis, this disruption is manifested through the loss of farmlands and the depletion of other green spaces [73]. In the same vein, the 2010–2013 Spatial Development Plan of the Sekondi-Takoradi Metropolitan Area ascribes the swift decline of green spaces to infrastructure development, which has been partially influenced by the emergence of the oil industries [22,78].

With the Built-up class, its area coverage in 1991 was 10.56 km^2 (5.51 %), which then increased to 22.13 km^2 (11.55 %) in 2009. It further expanded to 38.98 km^2 (20.33 %) in 2016 and finally increased to 73.63 km^2 (38.42 %) in 2023 (Table 3). Based on the analyses of land cover changes over time, it is evident that built-up consistently increased. Between 1991 and 2009, the built-up area expanded by 11.57 km^2 (6.04 %), followed by a substantial increase of 16.85 km^2 (8.78 %) between 2009 and 2016, and a significant growth of 34.65 km^2 (18.09 %) from 2016 to 2023 (Table 4). Generally, from the period of 1991 to 2023, built-up expanded by 63.07 km^2 (32.1 %). An explanation for this can be attributed to the increasing demand for land for various constructional purposes driven by population growth. and the upsurge in economic activities, which are partially connected to the oil discovery. This correlation has been emphasized by the 2021 Population and Housing Census of Ghana [79] and is also supported by the works of Aduah & Mantey, [43], and Dadzie-paintsil & Mensah, [41]. Before the oil discovery, the population of the metropolis in 2000 was 359,363. However, following the oil discovery, the population increased to 559, 548 in 2010 [80]. This surge in population was accompanied by migrants seeking employment opportunities as well as a corresponding rise in land demand for residential, commercial, and industrial purposes [23] leading to the conversion of various land cover types into built-up. According to Mensah et al., [22] the heightened demand for land for housing, especially, in 2011 led to a prompt intervention by real estate developers, and this birthed out the construction of housing projects like the Takoradi oil village and the King City to accommodate the growing population. Further, most establishments in the hospitality sector especially hotels had facelifts and expanded their facilities to accommodate more guests, while new establishments also emerged to meet the needs of high-income expatriates from the oil industry who relocated to the city for varying duration of time [27]. Moreover, in 2010, the Department of Urban Road initiated a plan to develop alternative routes and to expand existing single-lane roads into double-lane roads in the city. This led to the construction of the Kansaworado bypass, now known as N1. However, the construction of this bypass resulted in the conversion of land cover types into impermeable surfaces ([23]; STMA, 2010). Also, the expansion of the Takoradi port, which commenced in November 2014 according to the Ghana Ports and Harbour (GPHA), affected approximately 53,000 hectares of arable land in New Takoradi and Poase (GPHA, 2016). These developments have contributed to the expansion of built-up areas.

The data presented in Table 3 and Table 4 demonstrate significant changes in land use and land cover classes. These changes, according to the annual rate of change (Fig. 5), shows that between 1991 and 2009, water and vegetation decreased annually by 0.06 km^2 and 0.58 km^2 respectively. However, an increased annual rate of change was observed in built-up by 0.64 km^2 within the same period. Between 2009 and 2016, there was a decline of 0.17 km^2 in water and 2.23 km^2 in vegetation each year, while built-up areas increased by 2.4 km^2 annually. Moreover, from the period 2016–2023, water and built-up increased annually by 0.04 km^2 and by 4.95 km^2 respectively whereas vegetation decreased by an annual rate of 4.99 km^2. Over the entire study period, water decreased annually by 0.06 km^2, vegetation decreased by 1.91 km^2 and built-up increased by 1.97 km^2 annually (Fig. 5).

Table 4
Trend of land use and land cover changes between 1991 and 2023.

A. Class	1991 (km^2)	2009 (km^2)	Change (km^2)	1991 (%)	2009 (%)	Change (%)
Water	3.38	2.21	−1.17	1.77	1.16	−0.61
Vegetation	177.72	167.32	−10.40	92.72	87.29	−5.43
Built-up	10.56	22.13	11.57	5.51	11.55	6.04
B. Class	2009 (km^2)	2016 (km^2)	Change (km^2)	2009 (%)	2016 (%)	Change (%)
Water	2.21	1.03	−1.18	1.16	0.54	−0.62
Vegetation	167.32	151.66	−15.66	87.29	79.13	−8.16
Built-up	22.13	38.98	16.85	11.55	20.33	8.78
C. Class	2016 (km^2)	2023 (km^2)	Change (km^2)	2016 (%)	2023 (%)	Change (%)
Water	1.03	1.30	0.27	0.54	0.68	0.14
Vegetation	151.66	116.73	−34.93	79.13	60.90	−18.23
Built-up	38.98	73.63	34.65	20.33	38.42	18.09
D. Class	1991 (km^2)	2023 (km^2)	Change (km^2)	1991 (%)	2023 (%)	Change (%)
Water	3.38	1.30	−2.08	1.77	0.68	−1.09
Vegetation	177.72	116.73	−60.99	92.72	60.90	−31.82
Built-up	10.56	73.63	63.07	5.51	38.42	32.91

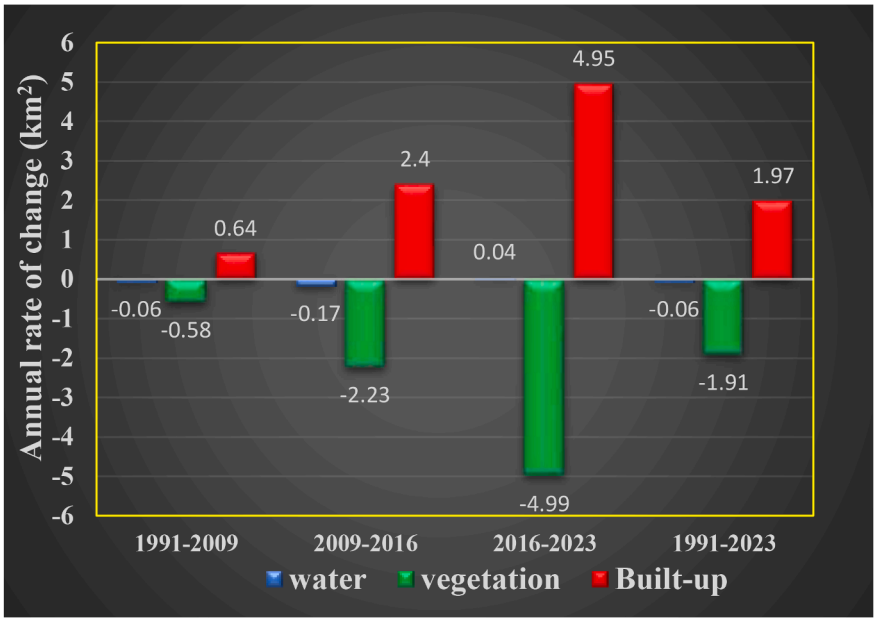

Fig. 5. Annual rate of change from 1991 to 2023.

Accuracy assessment of LULC classification

To assess the accuracy of the classified images, the error matrix and Kappa statistic were employed [5]. It was observed from Table 5 that an overall accuracy of 96.00 % was obtained for the year 2023. Correspondingly, the overall accuracy for the year 2016 was 94.67 %, 2009 was 90.67 %, and that of 1991 was 87.67 %. A Kappa coefficient of 0.82 was attained for 1991, 0.86 for 2009, 0.92 for 2016, and 0.94 for 2023. It is worth noting that the overall accuracy values presented in Table 5 exceeded the minimum 85 % accuracy standard proposed by Siddiqui et al., [81], Sarica et al., [82], and Krishnaveni & Anil, [5]. Therefore, the classification results can be used for further computation and analysis specifically, change detection analysis.

Transition probability

To gain deeper insights into the transformations that have occurred in the Sekondi-Takoradi Metropolis between 1991 and 2023, the change detection matrices depicted in Table 6 as well as the map of the transition matrices in Fig. 6 provided a comprehensive breakdown of the land use and land cover (LULC) categories within the metropolis. From Table 6, the columns represent the land cover classes of the later date and the rows indicate the land cover classes of the earlier date. The diagonal elements of the transition matrices show the classes that have not changed between the earlier dates and the later dates. However, the off-diagonals of the transition matrices indicate changes that have occurred in the classes from the earlier dates to the later dates.

Between 1991 and 2009, it can be observed from Table 6 that 1.40 km^2, 164.75 km^2, and 9.10 km^2 of water, vegetation, and built-up respectively did not change. These unchanged classes covered a total of 175.25 km^2 (91.43 %) while the classes that changed covered a total of 16.41 km^2 (8.56 %). Of the transition that occurred among the land cover classes, the conversion from vegetation to built-up was the highest with an area of 12.22 km^2 while the conversion from built-up to water had the least transition of 0.06 km^2. The increasing change in vegetation to built-up is by dint of increasing anthropogenic activities that occurred through the infrastructural development. This is proven in Table 6 where the rise in built-up at a rate of 11.57 km^2 was substantially from 10.41 km^2 decrease in vegetation and 1.17 km^2 loss in water.

From 2009 to 2016, the total land cover classes that remained unchanged covered an area of 170.38 km^2 (88.89 %) and the total land cover types that changed occupied an area of 21.26 km^2 (11.10 %). The unchanged area, in contrast to the transitional phase

Table 5
Assessment of classification accuracy.

Year	Producer's Accuracy			User's Accuracy			Overall Accuracy (%)	Kappa Coefficient
	Water	Vegetation	Built-up	Water	Vegetation	Built-up		
1991	88.66	86.41	88.00	86.00	89.00	88.00	***87.67***	***0.82***
2009	91.84	87.74	92.71	90.00	93.00	100	***90.67***	***0.86***
2016	94.06	93.20	96.88	95.00	96.00	93.00	***94.67***	***0.92***
2023	96.04	94.23	97.89	97.00	98.00	93.00	***96.00***	***0.94***

Table 6
Transition area matrices of various LULC from 1991 to 2023.

2009					
	LULC Class	Water (km^2)	Vegetation (km^2)	Built-up (km^2)	Total of 1991
1991	Water	**1.40**	1.17	0.81	**3.38**
	Vegetation	0.75	**164.75**	12.22	**177.72**
	Built-up	0.06	1.40	**9.10**	**10.56**
	Total of 2009	**2.21**	**167.32**	**22.13**	
Net change		***−1.17***	***−10.41***	**11.57**	
Total unchanged		***175.25 (91.43 %)***			
2016					
	LULC Class	Water (km^2)	Vegetation (km^2)	Built-up (km^2)	Total of 2009
2009	Water	**0.99**	0.79	0.43	**2.21**
	Vegetation	0.01	**149.08**	18.24	**167.32**
	Built-up	0.03	1.79	**20.31**	**22.13**
	Total of 2016	**1.03**	**151.66**	**38.98**	
Net change		***−1.18***	***−15.67***	***16.85***	
Total unchanged		***170.38 (88.89 %)***			
2023					
	LULC Class	**Water (km^2)**	Vegetation (km^2)	Built-up (km^2)	Total of 2016
2016	**Water**	**0.99**	0.00	0.04	**1.03**
	Vegetation	**0.10**	**116.02**	35.54	**151.66**
	Built-up	**0.21**	0.71	**38.05**	**38.98**
	Total of 2023	**1.30**	**116.73**	**73.63**	
Net change		***0.27***	***−34.93***	***34.66***	
Total unchanged		***155.06 (80.90 %)***			
2023					
	LULC Class	Water (km^2)	Vegetation (km^2)	Built-up (km^2)	Total of 1991
1991	Water	**1.19**	0.58	1.61	**3.38**
	Vegetation	0.08	**115.93**	61.71	**177.2**
	Built-up	0.03	0.22	**10.31**	**10.56**
	Total of 2023	**1.30**	**116.73**	**73.63**	
Net change		***−2.08***	***−60.99***	***63.08***	
Total unchanged		***127.42(66.48 %)***			

between 1991 and 2009 experienced a reduction of 4.87 km^2. Of the transitions that occurred among the land cover classes, the conversion from vegetation to built-up was the highest with an area of 18.24 km^2 while the conversion from vegetation to water had the least transition of 0.01 km^2. Lastly, the significant increase in built-up at a rate of 16.85 km^2 was mostly from 15.67 km^2 decrease in vegetation and 1.18 km^2 marginal decline in water (Table 6). Between 2016 and 2023, the total land use classes that remained unchanged was 155.06 km^2 (80.90 %) while the total area of classes that changed was 36.60 km^2 (19.10 %). The unchanged area, when compared to the transition period of 2009 and 2016, decreased by 15.32 km^2 (Table 6). This led to an increase in the area coverage of classes that changed by 15.32 km^2. Further, amid the transitions observed from the period 2016 to 2023, the conversion from vegetation to built-up was the highest with an area of 35.54 km^2 while the conversion from water to vegetation was the lowest with no change. Notably, water and built-up respectively increased by 0.27 km^2 and 34.66 km^2 and this was at the drastic decline in vegetation by 34.93 km^2 (Table 6). From the result, vegetative land has been increasingly converted to built-up and this is a visible indication of degradation of vegetation quality.

Generally, between 1991 and 2023, the total land use classes that remained unchanged was 127.42 km^2 (66.48 %) while the total area of classes that changed was 64.24 km^2 (33.52 %) (Table 6). Further, amid the transitions observed from the period between 1991 and 2023, the conversion from vegetation to built-up was the highest with an area of 61.71 km^2 while the conversion from built-up to water was the lowest with an area of 0.03 km^2 (Table 6). Remarkably, built-up increased by 63.08 km^2 and this was at the considerable decline in vegetation by 60.99 km^2 (Table 6). This analysis underscores the increasing trend of converting vegetative land into built-up areas, highlighting a visible degradation in vegetation quality.

Spatial variables

After thoroughly analyzing the land use and growth pattern of the metropolis, factors that influence changes in land cover and urban growth were assessed. According to Aduah et al., [83], how land is used in the Sekondi-Takoradi Metropolis and its surrounding areas is significantly influenced by some spatial variables such as elevation, slope, proximity to roads, and proximity to the Central business district (CBD) as depicted in Fig. 7.

To facilitate meaningful comparisons within the same range, the continuous raster maps were normalized using the minimum-maximum linear transformation technique [81], as depicted in Fig. 8.

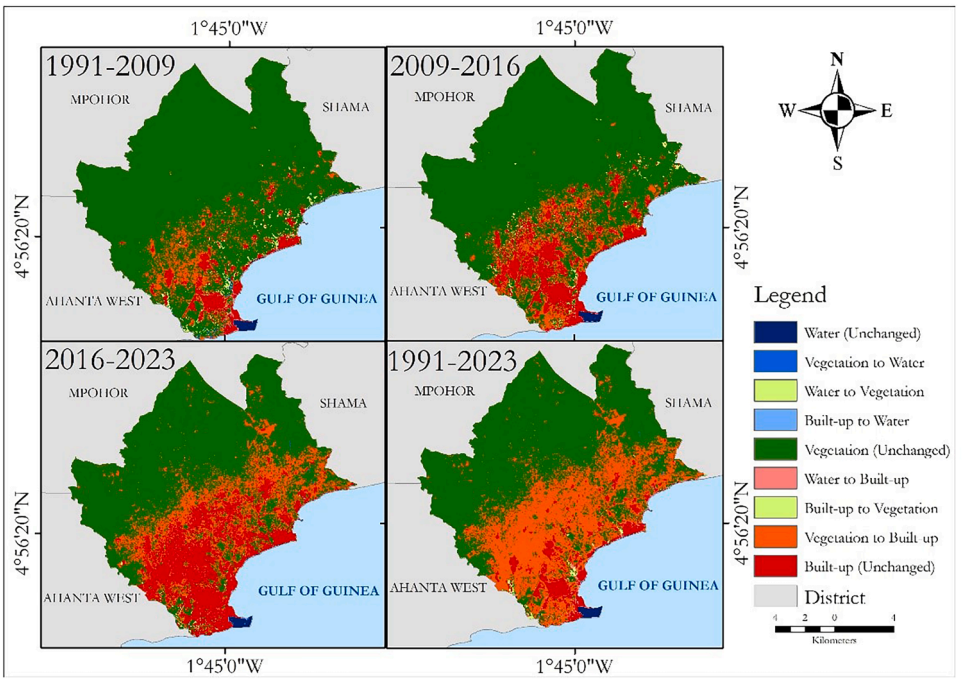

Fig. 6. Map of transition matrices (1991–2009, 2009–2016, 2016–2023, and 1991–2023).

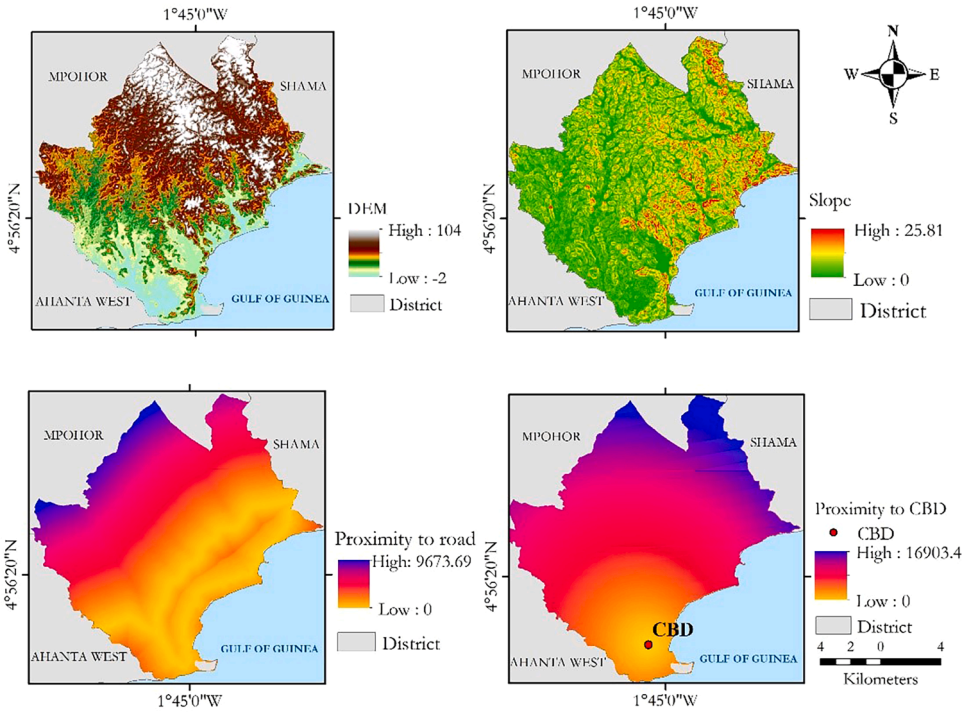

Fig. 7. spatial variables Elevation(a), Slope(b), Proximity to major roads (c), Proximity to CBD (d).

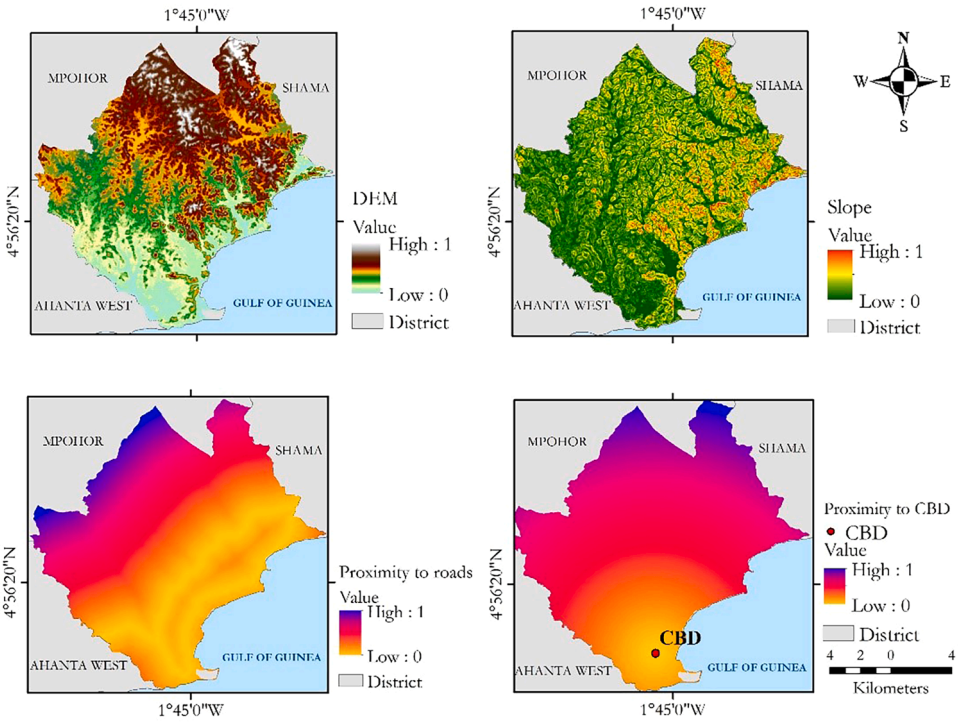

Fig. 8. Normalized spatial variables Elevation(a), Slope(b), Proximity to major roads (c), Proximity to CBD (d).

Simulation and projection of land use and land cover map

To forecast the future trend of land use and land cover in the study area, first, the 2009 and 2016 images were used to stimulate 2023 classified images by employing the cellular automated-based approach as shown in Fig. 9. Based on the stimulated 2023 classified image, water covered an area of 1.30 km^2 (0.68 %), vegetation covered a land size of 95.31 km^2 (49.73 %), and Built-up had an area of 95.05 km^2 (49.59 %) (Table 7). Comparing the area statistics of the simulated 2023 classified images to the actual 2023 classified image in Table 8, the area of water reduced by 0.01 Km^2, vegetation reduced by 0.71 Km^2, and built-up increased by 0.71 km^2. From Table 7, the stimulated 2023 classified image almost perfectly modelled the actual 2023 classified image with less than 1 % variations which are insignificant according to Rana & Sarkar, [36]. Therefore, the stimulated image was closely related to the actual 2023 image.

According to Satya et al., [37], predicting a land use and land cover is deemed reliable only when it is validated against the existing data. Therefore, the simulated 2023 image was validated with the actual classified 2023 image in Fig. 4 and 9. To determine the accuracy of the simulated 2023 image, four kappa statistics parameters namely; percent correctness, kappa location, kappa histogram, and overall kappa were computed (Table 8).

Kappa (location) is used to assess the simulation's capacity to detect location while Kappa (overall) is used to assess the overall performance of the simulation [37]. Kappa coefficient of 0 means no agreement exist between simulated and actual images whereas 1 means a perfect agreement. From Table 8, there exists a significant agreement between the simulated and actual 2023 LULC and that the model is good and reliable for predicting future land use and land cover of 2030. As the validation yielded a good agreement, the same process was used to project 2030 land use and land cover. The projected 2030 land use and land cover is shown in Fig. 10 with its area statistics of all classes in Table 9.

The selection of the year 2030 for projecting land use and land cover changes aligns with the strategic pursuit of the eleventh Sustainable Development Goal (SDG) which aims to "make cities and human settlements inclusive, safe, resilient, and sustainable" by 2030 [33,84]. According to Fig. 10, water is expected to decrease to 1.21 km^2 (0.63 %), vegetation is expected to 95.31 km^2 (49.73 %) and

Table 7
Area statistics of simulated 2023 and actual 2023 land use and land cover.

Simulated 2023 LULC			Actual 2023 LULC			Difference (A-S)
Class	Area (km^2)	%	Class	Area (km^2)	%	Area% (km^2)
Water	1.29	0.67	Water	1.30	0.68	−0.01 0.76
Vegetation	116.02	60.53	Vegetation	116.73	60.90	−0.71 0.61
Built-up	74.35	38.79	Built-up	73.63	38.42	+0.72 0.97
Total	**191.66**	**100**	**Total**	**191.66**	**100**	

S = Stimulated 2023 LULC and A = Actual 2023 LULC.

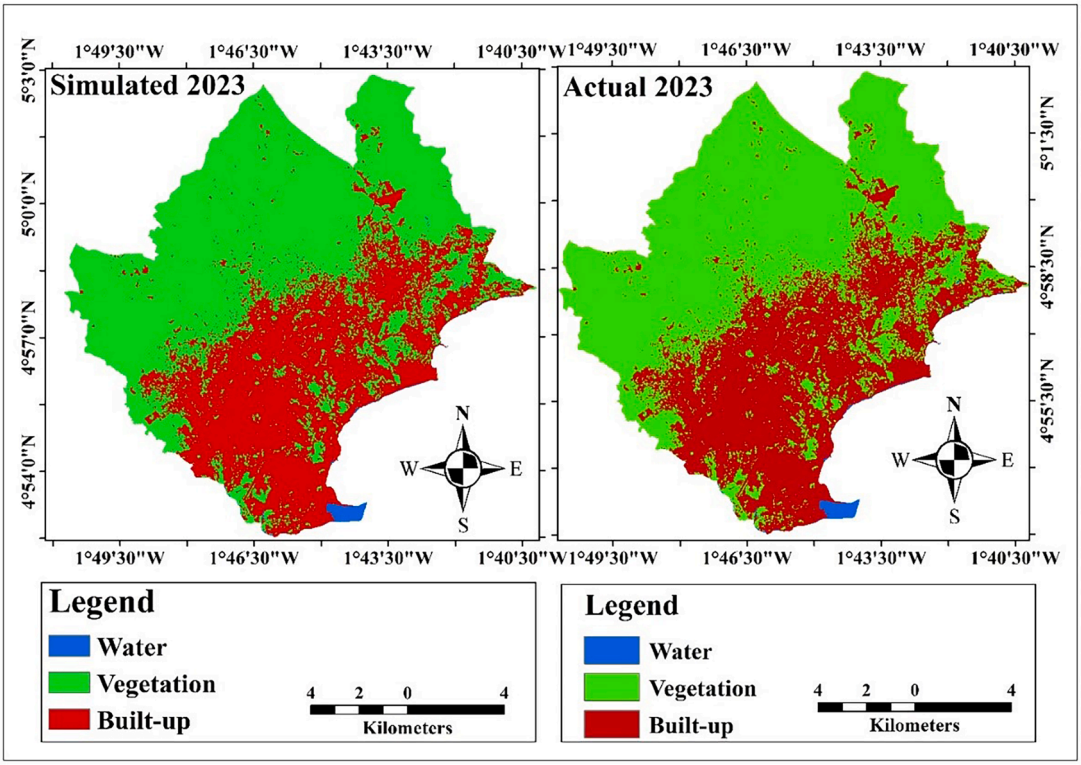

Fig. 9. Simulated and Actual 2023 land use and land cover map.

Table 8
Kappa index for simulated 2023 LULC with actual 2023 as reference.

Parameters	Value
Kappa (overall)	0.97
Kappa (histogram)	0.99
Kappa (location)	0.96
% of correctness	99.88

built-up will go up to 95.14 km^2 (49.64 %) (Table 9). The output of Fig. 10 shows that a significant conversion of other classes to built-up will mostly take place in the Western and South-Western parts of the metropolis. The Western part of the metropolis borders the Ahanta West district (Fig. 1; [22]), and the operational sites of most oil companies in the Ahanta West district is also closer to the Western and South-western part of the metropolis [22]. Therefore, these operational sites of oil companies serve as a pull factor for settlement and infrastructural development which may be a reason for higher conversion of other classes into built-up at the Western and the South-western parts of the metropolis. Moreover, in the South-western part of the metropolis is located the Takoradi airport, market circle, the Takoradi Harbour, companies, and the central business district. These infrastructural developments and places are mostly known for their influence on population increase which brings increasing demand for land for residential, industrial, and commercial purposes [25,85]. The projected pattern of built-up rapidly converting significant land covers like vegetation and water aligns with findings from various urbanization studies conducted in developing countries [5,28,31,45,57]. Therefore, for the metropolis to circumvent the irreversible challenges experienced by many cities, due to the increase in built-up, the metropolis must transition from its current business model and swiftly embrace an ecosystem-based approach to urban development as suggested by [32].

Lastly, in assessing how different the projected 2030 map will be from the classified 2023 map, it was revealed that water and vegetation will respectively decrease by 0.09 km^2 and 21.42 km^2 while built-up will increase by 21.51 km^2. The decrease in water and vegetation will occur at an annual rate of 0.01 km^2 and 3.06 km^2 whereas built-up will increase annually at a rate of 3.07 km^2 (Table 10). This means the metropolis is becoming more urbanized and will continue in the development of new infrastructures as evidenced in Table 9. However, as indicated by Abudu et al., [45], the metropolis must attain a sustainable balance that can manage infrastructure development, population growth, and environmental preservation as it expands because the increase in impervious surfaces at the expense of natural vegetation, water, and proper planning makes a city or an urban area susceptible to urban flooding and urban heat which affect the quality and survival of life in the urban environmental [21,59].

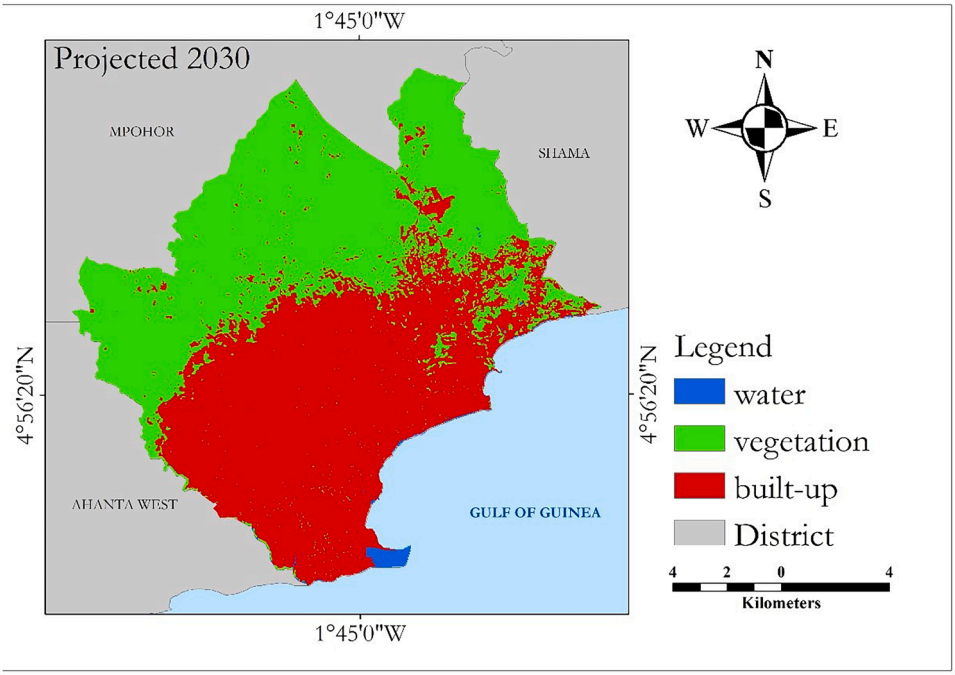

Fig. 10. Projected LULC map of 2030.

Table 9
Area statistics of Projected 2030 land use and land cover.

Class	Area (km^2)	%
Water	1.21	0.63
Vegetation	95.31	49.73
Built-up	95.14	49.64
Total	**191.66**	**100**

Table 10
Change detection between 2023 LULC and Predicted 2030.

LULC Class	2023 (km^2)	2030 (km^2)	Area (km^2)	Percentage Change (%)	Annual change rate (km^2)
Water	1.30	1.21	−0.09	−6.92	−0.01
Vegetation	116.73	95.31	−21.42	−18.35	−3.06
Built-up	73.63	95.14	21.51	29.21	3.07

Conclusion

The study employed Landsat images to analyze the spatio-temporal dynamics of land use and land cover within the Sekondi-Takoradi metropolis from 1991 to 2023. The land use and land cover dynamics were examined by classifying the Landsat images into three categories: water, vegetation, and built-up areas through the use of random forest classification method. Notably, the most significant class conversion observed during this period was the depletion of vegetation, with a substantial portion of 60.99 km^2 converted into built-up land. The study, further showed that the metropolis has expanded its sphere of influence greatly to the south and south-western boundary by annexing nearby towns and communities over the last three decades. The methodology employed in this study can be adapted to assess changes in the land cover in other metropolises in Ghana or similar developing countries. Understanding the changes in land use and land cover is vital for achieving the Sustainable Development Goal of creating inclusive, safe, resilient, and sustainable urban environments. Decision-makers, urban planners, and policymakers can leverage these findings to address inadequately enforced land-use regulations and develop effective plans, strategies, and policies to optimize resource and infrastructure allocation. However, to enhance the accuracy of the findings, further research is needed to encompass other aspects of urban sprawl dynamics, such as its various drivers and a landscape metrics analysis in different directions.

Author statement

All authors played a crucial role in shaping the concept of the study.

Funding

This study was funded by the West African Science Service Centre on Climate Change and Adapted Land Use (WASCAL).

Declarations ethical approval

Not applicable.

CRediT authorship contribution statement

Ernest Biney: Conceptualization, Formal analysis, Methodology, Writing – original draft, Writing – review & editing. **Eric Kwabena Forkuo:** Supervision, Writing – review & editing, Conceptualization. **Michael Poku-Boansi:** Supervision, Writing – review & editing. **Yaw Mensah Asare:** Methodology, Supervision, Writing – review & editing. **Kwame O. Hackman:** Supervision, Software, Writing – review & editing. **Daniel Buston Yankey:** Software, Methodology, Visualization. **Albert Elikplim Agbenorhevi:** Writing – review & editing, Visualization. **Ernestina Annan:** Methodology, Writing – review & editing.

Declaration of competing interest

The authors declare that they have no known competing financial interests or personal relationships that could have appeared to influence the work reported in this paper.

Acknowledgments

My heartfelt gratitude goes to the Federal Ministry of Education and Research (BMBF) and the West African Science Centre on Climate Change and Adapted Land Use (WASCAL) for awarding me the scholarship that supported my PhD research, which led to the creation of this publication.

References

[1] A. Younes, A. Ahmad, A.D. Hanjagi, A.M. Nair, Understanding dynamics of land use & land cover change using GIS & change detection techniques in Tartous, Syria 14 (3) (2023) 20–41, https://doi.org/10.48088/ejg.a.you.14.3.020.041.
[2] H. Mohammadian, J. Tavakoli, H. Khani, Monitoring land use change and measuring urban sprawl based on its spatial forms The case of Qom city, Egypt. J. Remote Sens. Space Sci. 20 (1) (2017) 103–116, https://doi.org/10.1016/j.ejrs.2016.08.002.
[3] J. Obodai, K. Amaning, S. Nii, M. Lumor, Land use /land cover dynamics using landsat data in a gold mining basin-the, Remote Sens. App.: Soc. Environ. 13 (October 2018) (2019) 247–256, https://doi.org/10.1016/j.rsase.2018.10.007.
[4] M.S. Ramadan, H.A. Effat, Geospatial modeling for a sustainable urban development zoning map using AHP in Ismailia Governorate, Egypt, Egypt. J. Remote Sens. Space Sci. 24 (2) (2021) 191–202, https://doi.org/10.1016/j.ejrs.2021.01.003.
[5] K.S. Krishnaveni, P.P. Anil, Spatio-temporal dynamics of urban sprawl in a rapidly urbanizing city using machine learning classification, Geocarto Int 37 (27) (2022) 17403–17434, https://doi.org/10.1080/10106049.2022.2129817.
[6] T.K.C.N. Thambawita, D.S. Munasinghe, L.K.K. Yapa, Identification of Urban Heat Island Effect on Land Use Land Cover Changes, J. Geospatial Survey. 3 (2) (2023) 43–53, https://doi.org/10.4038/jgs.v3i2.50.
[7] K. Abass, G. Dumedah, F. Frempong, A.S. Muntaka, D.O. Appiah, E.K. Garsonu, R.M. Gyasi, Rising incidence and risks of floods in urban Ghana : is climate change to blame ? Cities. 121 (September 2021) (2022) 103495 https://doi.org/10.1016/j.cities.2021.103495.
[8] J.L. Rainey, S.D. Brody, G.E. Galloway, W.E. Highfield, J.L. Rainey, S.D. Brody, G.E. Galloway, W.E. Highfield, Assessment of the growing threat of urban flooding : a case study of a national survey, Urban. Water. J. 00 (00) (2021) 1–7, https://doi.org/10.1080/1573062X.2021.1893356.
[9] B.F. Frimpong, Land Use and Cover Changes in the Mampong Municipality of the Ashanti Region, Kwame Nkrumah University 0f Science and Technology, Kumasi, 2015.
[10] L.T. Phong, Analysis of Forest Cover Dynamics and Their Driving Forces in Bach Ma National Park and Its Buffer Zone Using Remote Sensing and GIS, International Institute fro Geo-information and Earth Observation, Enschede, The Netherlands, 2004.
[11] M.S. Aduah, P.E. Baffoe, Remote sensing for mapping land-use /cover changes and urban sprawl in sekondi-takoradi, Western Region Ghana (2013) 66–73.
[12] K. Getu, H.G. Bhat, Analysis of spatio-temporal dynamics of urban sprawl and growth pattern using geospatial technologies and landscape metrics in Bahir Dar, Northwest Ethiopia, Land Use Policy 109 (August) (2021) 105676, https://doi.org/10.1016/j.landusepol.2021.105676.
[13] Z. Alijani, F. Hosseinali, A. Biswas, Spatio-temporal evolution of agricultural land use change drivers: a case study from Chalous region, Iran, J. Environ. Manage. 262 (June 2019) (2020) 110326, https://doi.org/10.1016/j.jenvman.2020.110326.
[14] S. Alqadhi, J. Mallick, S. Talukdar, A.A. Bindajam, A.A.A. Shohan, Quantification of Urban Sprawl for Past-To-Future in Abha City, Saudi Arabia Quantification of Urban Sprawl for Past-To-Future in Abha City,. August, Comput. Modell. Eng. Sci. (2021), https://doi.org/10.32604/cmes.2021.016640.
[15] Han, H., Yang, C., & Song, J. (2015). *Scenario simulation and the prediction of land use and land cover change in Beijing, China*. 4260–4279. https://doi.org/10.3390/su7044260.
[16] N. Varghese, N.P. Singh, Land Use Policy Linkages between land use changes, desertification and human development in the Thar Desert Region of India, Land Use Policy 51 (2016) 18–25, https://doi.org/10.1016/j.landusepol.2015.11.001.
[17] F. Mukherjee, D. Singh, Assessing Land Use – land cover change and its impact on land surface temperature using LANDSAT Data : a Comparison of Two Urban Areas in India, *Earth Syst. Environ., 0123456789* (2020), https://doi.org/10.1007/s41748-020-00155-9.
[18] S. Saha, A. Saha, M. Das, A. Saha, R. Sarkar, A. Das, Analyzing spatial relationship between land use /land cover (LULC) and land surface temperature (LST) of three urban agglomerations (UAs) of Eastern India, Remote Sens. Appl.: Soc. Environ. 22 (April) (2021) 100507, https://doi.org/10.1016/j.rsase.2021.100507.

[19] K. Frimpong, D. Eugene, E.J.Van Etten, Urban sprawl and microclimate in the Ga East municipality of Ghana, Heliyon. 8 (March) (2022) 09791, https://doi.org/10.1016/j.heliyon.2022.e09791.
[20] C. Nyamekye, S. Kwofie, B. Ghansah, E. Agyapong, L. Appiah, Assessing urban growth in Ghana using machine learning and intensity analysis : a case study of the New Juaben Municipality, Land Use Policy 99 (August) (2020) 105057, https://doi.org/10.1016/j.landusepol.2020.105057.
[21] B. Doe, C. Amoako, R. Adamtey, Spatial expansion and patterns of land use/land cover changes around Accra, Ghana – Emerging insights from Awutu Senya East Municipal Area, Land use policy 112 (August 2021) (2022) 105796, https://doi.org/10.1016/j.landusepol.2021.105796.
[22] C.A. Mensah, J.K. Eshun, Y. Asamoah, E. Ofori, Changing land use /cover of Ghana ' s oil city (Sekondi-Takoradi Metropolis): implications for sustainable urban development, Int J Urban Sustain Dev 11 (2) (2019) 223–233, https://doi.org/10.1080/19463138.2019.1615492.
[23] R.E. Fiave, Sekondi-Takoradi as an Oil City 37 (1) (2017) 61–79.
[24] N. Alqattan, M. Acheampong, F.M. Jaward, N. Vijayakumar, L. Ebude, D. Enomah, Evaluation of the potential hydrological impacts of land use /cover change dynamics in Ghana ' s oil city, *Environ., Dev. Sustain., 0123456789* (2019), https://doi.org/10.1007/s10668-019-00507-0.
[25] Vinh, T., & Nguyen, D. (2019). *Transcalar Urban Governance : Planning and Development in the " Oil-City " of Sekondi-Takoradi, Ghana*.
[26] United Nations. Sustainable development goals, Unit, 2015. https://sustainabledevelopment.un.org/.
[27] E. Biney, E. Boakye, Urban sprawl and its impact on land use land cover dynamics of Sekondi-Takoradi metropolitan assembly, Ghana, Environ. Challeng. 4 (April) (2021) 100168, https://doi.org/10.1016/j.envc.2021.100168.
[28] K.O. Hackman, X. Li, D. Asenso-gyambibi, A. Emmanuella, I.D. Nelson, Analysis of geo-spatiotemporal data using machine learning algorithms and reliability enhancement for urbanization decision support, Int. J. Digit. Earth. 0 (0) (2020) 1–16, https://doi.org/10.1080/17538947.2020.1805036.
[29] Juma, A., Gudo, A., Deng, J., & Qureshi, A.S. (2022). *Analysis of spatiotemporal dynamics of land use /cover changes in Jubek State, South Sudan*.
[30] E.P.P. Manesha, A. Jayasinghe, H. Nawod, Measuring urban sprawl of small and medium towns using GIS and remote sensing techniques : a case study of Sri Lanka, Egypt. J. Remote Sens. Space Sci. 24 (3) (2021) 1051–1060, https://doi.org/10.1016/j.ejrs.2021.11.001.
[31] A. Tariq, J. Yan, F. Mumtaz, Land change modeler and CA-Markov chain analysis for land use land cover change using satellite data of Peshawar, Pakistan, Phys. Chem. Earth. 128 (October) (2022) 103286, https://doi.org/10.1016/j.pce.2022.103286.
[32] S. Wangyel, L. Munkhnasan, W. Lee, Land use and land cover change detection and prediction in Bhutan ' s high altitude city of Thimphu, using cellular automata and Markov chain, Environ. Challeng. 21 (November 2020) (2021) 100017, https://doi.org/10.1016/j.envc.2020.100017.
[33] Z. Shao, N.S. Sumari, A. Portnov, F. Ujoh, P.J. Mandela, Geo-spatial Information Science Urban sprawl and its impact on sustainable urban development : a combination of remote sensing and social media data, Geo-Spatial Inf. Sci. 24 (2) (2021) 241–255, https://doi.org/10.1080/10095020.2020.1787800.
[34] K. Dissanayake, in: Ecological Evaluation of Urban Heat Island Effect in Colombo City, Sri Lanka Based on Landsat 8 Satellite Data, IEEE, 2020, pp. 531–536.
[35] M. Hasan, R. Haque, M. Rahman, Identifying the land use land cover (LULC) changes using remote sensing and GIS approach : a case study at Bhaluka in Mymensingh, Bangladesh, Case Stud. Chem. Environ. Eng. 7 (December 2022) (2023) 100293, https://doi.org/10.1016/j.cscee.2022.100293.
[36] S. Rana, S. Sarkar, Prediction of urban expansion by using land cover change detection approach, Heliyon. 7 (August) (2021) e08437, https://doi.org/10.1016/j.heliyon.2021.e08437.
[37] B.A. Satya, M. Shashi, D. Pratap, Future land use land cover scenario simulation using open source GIS for the city of Warangal, Telangana, India, Appl. Geomat. (2020), https://doi.org/10.1007/s12518-020-00298-4. Springer 2011.
[38] Rangarajan, S. (2022). *Predicting the Future Land Use and Land Cover Changes for Bhavani Basin, Tamil Nadu, India Using QGIS MOLUSCE Plugin*.
[39] STMA. (2022). *SEKONDI-TAKORADI METROPOLITAN ASSEMBLY MEDIUM-TERM DEVELOPMENT PLAN. June 2021*.
[40] Service, G.S. (2014). 2010 Population and housing census report, *Ghana Statistical Service*.
[41] Dadzie-paintsil, E., & Mensah, J.V. (2022). *Effects of urbanization on coastal wetlands in the Sekondi-Takoradi Metropolis, Ghana*. 6(2), 94–105. https://doi.org/10.13057/oceanlife/o060205.
[42] Ghana Statistical Service. *2010 POPULATION & Ghana Statistical Service (2010). 2010 POPULATION & HOUSING CENSUS REPORT.*, 2010.
[43] M.S. Aduah, S. Mantey, Assessment of land use efficiencies of Ghanaian Cities: case study of sekondi-takoradi metropolis, South Afr. J, Geom. 12 (1) (2023) 86–97, https://doi.org/10.4314/sajg.v12i1.6.
[44] M. Gašparović, Urban Growth Pattern Detection and Analysis, Urban Ecol. (2020) 35–48, https://doi.org/10.1016/B978-0-12-820730-7.00003-3.
[45] D. Abudu, R. Azo, G. Andogah, Spatial assessment of urban sprawl in Arua Municipality, Uganda, Egypt. J. Remote Sens. Space Sci. 22 (3) (2019) 315–322, https://doi.org/10.1016/j.ejrs.2018.01.008.
[46] K. Abass, S.K. Adanu, R.M. Gyasi, Urban sprawl and land use /land-cover transition probabilities in peri-urban Kumasi, Ghana, West Afr. J. Appl. Ecol. 26 (2018) 118–132.
[47] Kombate A., Folega, F., Atakpama, W., Dourma, M., Wala, K., & Goïta, K. (2022). *Characterization of land-cover changes and forest-cover dynamics in Togo between 1985 and 2020 from Landsat Images Using Google Earth Engine*. 1–34.
[48] N. Ullah, A.M. Siddique, M. Ding, S. Grigoryan, T. Zhang, Y. Hu, Spatiotemporal Impact of Urbanization on Urban Heat Island, Buildings MPDI, (2022) 21–23.
[49] M. Fernández-Delgado, Do we need hundreds of classifiers to solve real world classification problems? The Journal of Machine Learning Research 15 (1) (2014) 3133–3181.
[50] N. Horning. Random Forests : An algorithm for image classification and generation of continuous fields data sets, 2010.
[51] O.O. Othow, S.L. Gebre, D. Gemeda, Analyzing the rate of land use and land cover change and determining the causes of forest cover change in gog district, Gambella Regional (2017), https://doi.org/10.4172/2469-4134.1000219.
[52] Foody, G.M. (2020). Explaining the unsuitability of the kappa coefficient in the assessment and comparison of the accuracy of thematic maps obtained by image classification. *Remote Sens. Environ.*, 239(August 2019), 111630. https://doi.org/10.1016/j.rse.2019.111630.
[53] D. García-álvarez, M. Teresa, C Olmedo, in: D. García-Álvarez, M. Paegelow, M.T.C. Olmedo, J.F. Mas (Eds.), Land Use Cover Datasets and Validation Tools, Springer International Publishing, 2022, https://doi.org/10.1007/978-3-030-90998-7 (eds.).
[54] M. Shamsudeen, R. Padmanaban, P. Cabral, P. Morgado, Spatio-Temporal Analysis of the Impact of Landscape Changes on Vegetation and Land Surface Temperature over Tamil Nadu, MDPI 3 (2022) 614–638.
[55] M.H. Elagouz, S.M. Abou-shleel, A.A. Belal, M.A.O. El-mohandes, Detection of land use /cover change in Egyptian Nile Delta using remote sensing, Egypt. J. Remote Sens. Space Sci. 23 (1) (2020) 57–62, https://doi.org/10.1016/j.ejrs.2018.10.004.
[56] Stemn, E., & Agyapong, E. (2014). Assessment of Urban Expansion in the Sekondi-Takoradi Metropolis of Ghana Using Remote-Sensing and GIS Approach. 3(8).
[57] Y.M. Asare, I. Selby, G. Ashiagbor, C.Y. Asante, Analysis and prediction of land use land cover dynamics in the Kpeshie Lagoon Basin of Ghana using satellite remote sensing, J. Ghana Inst. Eng. 23 (1) (2023).
[58] K.T. Deribew, Spatiotemporal analysis of urban growth on forest and agricultural land using geospatial techniques and Shannon entropy method in the satellite town of Ethiopia, the western fringe of Addis Ababa city, Ecol. Process. 9 (1) (2020) 46.
[59] S. Hussain, M. Mubeen, S. Karuppannan, Land use and land cover (LULC) change analysis using TM, ETM + and OLI Landsat images in district of Okara, Punjab, Pakistan, Phys. Chem. Earth. 126 (February 2021) (2022) 103117, https://doi.org/10.1016/j.pce.2022.103117.
[60] Nath, N., Sahariah, D., Meraj, G., Debnath, J., & Kumar, P. (2023). *Land use and land cover change monitoring and prediction of a UNESCO World Heritage Site : Kaziranga Eco-Sensitive*.
[61] Abdullahi, S., & Pradhan, B. (2017). Urban expansion and change detection analysis. *Spatial Modeling and Assessment of Urban Form: Analysis of Urban Growth: From Sprawl to Compact Using Geospatial Data*, 155-170.
[62] E. Boakye, F.O.K. Anyemedu, J.A. Quaye-Ballard, E.A. Donkor, Spatio-temporal analysis of land use/cover changes in the Pra River Basin, Ghana, Applied Geomatics 12 (2020) 83–93.
[63] N.R. Khwarahm, Spatial modeling of land use and land cover change in Sulaimani, Iraq, using multitemporal satellite data, Environ. Monit. Assess. 193 (3) (2021), https://doi.org/10.1007/s10661-021-08959-6.
[64] S. Gaur, S. Rajendra, A comprehensive review on land Use /land cover (LULC) change modeling for urban development : current status and future prospects, MDPI (2023), https://doi.org/10.3390/su15020903.

[65] D. Issiako, K. Soufiyanou, T.I. Ismaila, Prospective mapping of land cover and land use in the classified forest of the upper alibori based on satellite imagery, J. Geomat. Plann. (2022), https://doi.org/10.14710/geoplanning.8.2.115-126.
[66] A. Zaki, I. Buchori, A. Wahyu, Y. Liu, An object-based image analysis in QGIS for image classification and assessment of coastal spatial planning q, Egypt. J. Remote Sens. Space Sci. 25 (2) (2022) 349–359, https://doi.org/10.1016/j.ejrs.2022.03.002.
[67] Kumi-boateng, B., & Stemn, E. (2015). *Effect of Urban Growth on Urban Thermal Environment : A Case Study of Sekondi-Takoradi Metropolis of Ghana*. 5(2), 32–42.
[68] H.M. Mosammam, A.M. Mosammam, M. Sarrafi, J.T. Nia, H. Esmaeilzadeh, Analyzing the potential impacts of climate change on rainfed wheat production in Hamedan Province, Iran, via generalized additive models, J. Water Clim. Change 7 (1) (2017) 212–223.
[69] Aklorbortu, M.D., 2019. Floods take over Sekondi-Takoradi after heavy rains. Daily Graphic [online]. Available from: http://www.dailygraphic.com [Accessed 20 June 2022].
[70] S.Y. Danso, I.Y. Addo, Coping strategies of households affected by flooding : a case study of Sekondi-Takoradi Metropolis in Ghana, Urban. Water. J. (2018) 1–7, https://doi.org/10.1080/1573062X.2016.1176223.
[71] D.O. Appiah, Geoinformation Modelling of Peri-Urban Land Use and Land Cover Dynamics for Climate Variability and Climate Change in the Bosomtwe District, Ghana, 2016.
[72] E. Daata, E. Kwabena, E. Biney, E. Harris, J.A. Quaye-ballard, The impact of land use and land cover changes on socioeconomic factors and livelihood in the Atwima Nwabiagya district of the Ashanti region, Ghana, Environ. Challeng. 5 (July) (2021) 100226, https://doi.org/10.1016/j.envc.2021.100226.
[73] C.A. Mensah, K.V. Gough, D. Simon, Urban Green Spaces Grow Oil Cities : Case Sekondi-Takoradi 40 (4) (2018).
[74] Independent Oil and Gas Information centre (2017) Ghana's oil city: what investors are failing to see?, http://oilandgasirc.org.gh/news-posts/ghanas-oil-city-what-investors-are-failing-to-see/.
[75] K.V. Gough, P.W. Yankson, Land markets in African cities: the case of peri-urban Accra, Ghana, Urban studies 37 (13) (2000) 2485–2500.
[76] Yalley, P. P., & Ofori-Darko, J. (2012). The effects of Ghana‟ s oil discovery on land and house prices on communities nearest to the oil filed in Ghana (Case Study: Kumasi and Sekondi-Takoradi). In *Procs 4th West Africa Built Environment Research (WABER) Conference, 24–26 July 2012* (pp. 1443-1454).
[77] G. Ennis, M. Finlayson, G. speering, Expecting a boomtown? Exploring potential housing: related impacts of large scale resource developments in Darwin, Human Geogra- phies 7 (1) (2013) 33–42.
[78] STMA. Medium-Term Development Plan, Sekondi, Ghana: STMA, 2013.
[79] G.S. Service. Ghana 2021 population, and housing census, 2021.
[80] Ghana statistical services. 2010 population and housing census: summary of report of final results, Accra, sakoa Press, 2012.
[81] A. Siddiqui, A. Siddiqui, S. Maithani, A.K. Jha, P. Kumar, S.K. Srivastav, Urban growth dynamics of an Indian metropolitan using CA Markov and Logistic Regression, Egypt. J. Remote Sens. Space Sci. 21 (3) (2018) 229–236, https://doi.org/10.1016/j.ejrs.2017.11.006.
[82] G.M. Sarica, T. Zhu, Spatio-temporal dynamics of flood exposure in Shenzhen from present to future, Urban Anal. City Sci. 48 (5) (2021) 1011–1024, https://doi.org/10.1177/2399808321991540.
[83] M.S. Aduah, S. Mantey, T.M. Area, Modelling Potential Future Urban Land Use Changes in the Sekondi-Takoradi Metropolitan Area of Ghana, 2, 2020.
[84] K. Andersson, S. Dickin, A. Rosemarin, Towards " Sustainable " Sanitation : challenges and Opportunities in Urban Areas, Sustain., MDPI (2016), https://doi.org/10.3390/su8121289.
[85] P.W.K. Yankson, K.V. Gough, J. Esson, F. Ebenezer, Spatial and social transformations in a secondary city : the role of mobility in Sekondi-Takoradi, Ghana, Geografisk Tidsskrift-Danish J. Geogr. 7223 (2017) 1–11, https://doi.org/10.1080/00167223.2017.1343672.